0090-9556/00/2803-0315–322$02.00/0
DRUG METABOLISM AND DISPOSITION
Vol. 28, No. 3
Printed in U.S.A.

BIOSYNTHESIS OF ALL-*TRANS*-RETINOIC ACID FROM ALL-*TRANS*-RETINOL: CATALYSIS OF ALL-*TRANS*-RETINOL OXIDATION BY HUMAN P-450 CYTOCHROMES

HAO CHEN, WILLIAM N. HOWALD, AND MONT R. JUCHAU

Department of Pharmacology, School of Medicine (H.C., M.R.J.) and Department of Medicinal Chemistry, School of Pharmacy (W.N.H.), University of Washington, Seattle, Washington

(Received July 20, 1999; accepted November 22, 1999)

This paper is available online at http://www.dmd.org

ABSTRACT:

Oxidative conversion of all-*trans*-retinol (*t*-ROH) to all-*trans*-retinal (*t*-RAL) is recognized as the rate-limiting step for biosynthesis of all-*trans*-retinoic acid from *t*-ROH in mammalian hepatic tissues. The purpose of this study was to investigate the role of human cytochrome P-450 (CYP)-dependent monooxygenation in the conversion of *t*-ROH to *t*-RAL. Adult human liver microsomes (HLMS) were incubated with *t*-ROH, and retinoids generated were identified and quantified by liquid chromatography-mass spectroscopy, HPLC, and other methods. HLMS-catalyzed generation of *t*-RAL from *t*-ROH was primarily NADPH-dependent and was strongly inhibited by carbon monoxide. Rates of reactions increased linearly with time and concentrations of HLMS, and exhibited classical substrate saturation. These observations strongly indicated that the reaction proceeded via CYP-catalyzed monooxygenation. On the basis of responses to selective chemical inhibitors, isoforms from CYP family 1 and the CYP3A subfamily appeared to be very active. Members of the CYP2C subfamily and CYP2D6 exhibited lesser activities and CYP2A6, CYP2B6, and CYP2E1 were virtually inactive. cDNA-expressed human CYP enzymes (CYP SUPERSOMES) also were used to assess the capacity of individual CYP enzymes to catalyze the reaction. Based on responses to selective chemical inhibitors, specific activities, and levels present in adult human hepatic tissues, CYP1A2 and CYP3A4 strongly appeared to be the major CYP enzymes catalyzing hepatic oxidative conversion of *t*-ROH to *t*-RAL in the adult human liver. CYP1A1 and CYP1B1 SUPERSOMES both exhibited exceptionally high activities, and in extrahepatic tissues, these isoforms could play important roles in biosynthesis of all-*trans*-retinoic acid from *t*-ROH.

All-*trans*-retinoic acid (*t*-RA)[1], the highly receptor-active metabolite of all-*trans*-retinol (vitamin A_1, *t*-ROH), can trigger retinoid-mediated signal transduction pathways via binding to nuclear retinoic acid receptors (Petcovich et al., 1987; Means and Gudas, 1995). This *t*-RA-induced, retinoid receptor-mediated signal transduction is believed to be responsible for many if not all of the observed potent therapeutic and teratogenic effects of retinoids in humans (Soprano and Soprano, 1995).

Oxidative conversions of *t*-ROH directly control endogenous levels of *t*-RA and thus play an important role in retinoid receptor-mediated gene expression. Conversion of *t*-ROH to *t*-RA in adult hepatic tissues comprises two consecutive reactions (Kim et al., 1992; Napoli, 1996). *t*-ROH is first oxidized to all-*trans*-retinal (*t*-RAL), and the formed *t*-RAL is then rapidly oxidized to *t*-RA. It is generally agreed that, under normal conditions, the first reaction is the rate-limiting step and that its rate controls rates of biosynthesis of *t*-RA from *t*-ROH.

In hepatic tissues, the major metabolic site of retinoid biotransformation, it is well accepted that conversion of *t*-ROH to *t*-RAL can be catalyzed by alcohol dehydrogenase isoenzymes, and that subsequent conversion of *t*-RAL to *t*-RA is mainly catalyzed by aldehyde dehydrogenases (Blaner and Olson, 1994; Napoli, 1996; Duester, 1998). In rats, a microsomal retinol dehydrogenase also has been characterized (Napoli and Race, 1990; Napoli et al., 1992), and that enzyme catalyzes the conversion of retinol to retinal effectively. Recently, a human microsomal NAD^+-dependent dehydrogenase was identified as an efficient retinol dehydrogenase (Gough et al., 1998). Because these enzymes have shown low K_m (4–22 μM) and high V_{max}/K_m pmol/min/μM, it is widely accepted that these microsomal retinol dehydrogenases may play a major role in biosynthesis of *t*-RA from retinol in both rodent and human hepatic tissues.

Recent studies have demonstrated that various cytochrome P-450 (CYP)-dependent monooxygenases that are recognized as important xenobiotic-etabolizing enzymes, can also catalyze the second step in the biosynthesis of *t*-RA from *t*-ROH—the conversion of *t*-RAL to *t*-RA (Roberts et al., 1992; Raner et al., 1996). These findings are important because they suggest an alternative mechanism for endogenous generation of *t*-RA in addition to the alcohol dehydrogenase/ADLH-dependent pathways. Many CYP isoforms shown to catalyze the reaction are important drug-metabolizing enzymes and it thus seems likely that catalysis of retinoid biotransformation by CYP could result in significant drug-retinoid interactions. However, whether and to what extent CYP isoforms can catalyze conversion of *t*-ROH to *t*-RAL (the rate-limiting step) have not been reported to our knowledge.

This work was supported by National Institute of Environmental Health Sciences Grant ES-04041.

[1] Abbreviations used are: *t*-RA, all-*trans*-retinoic acid; *t*-ROH, all-*trans*-retinol; *t*-RAL, all-*trans*-retinal; HLMS, human liver microsomes; CYP, cytochrome P-450; ANF, α-naphthoflavone; TAO, troleandomycin; LC-MS, liquid chromatography-mass spectroscopy; CO, carbon monoxide.

Send reprint requests to: M. R. Juchau, Ph.D., Department of Pharmacology, School of Medicine, Box 357280, University of Washington, Seattle, WA 98185. E-mail: juchau@u.washington.edu

In an earlier study (Shih and Hill, 1991), it was reported that rat liver microsomes were able to catalyze conversion of retinol to retinal and the reaction was characterized as oxidase-dependent. However, the same reaction was also shown to be NADPH-dependent, sensitive to inhibition by ketoconazole and α-naphthoflavone (ANF), and was inducible by 3-methylcholanthrene. Those interesting observations suggested to us that the reaction was primarily, if not exclusively, catalyzed by P-450-dependent monooxygenases rather than an oxidase(s). The importance of oxidation of *t*-ROH to *t*-RAL and the possible catalysis by CYP for the reaction appeared to warrant a rigorous and thorough investigation.

In this study, we investigated the potential for CYP-catalyzed oxidative conversion of *t*-ROH to *t*-RAL in adult human hepatic tissues. The objectives of this study were: 1) to investigate whether *t*-ROH can be oxidatively converted into *t*-RAL via a cytochrome P-450-catalyzed monooxygenation; and 2) if the P-450-dependent reactions proceeded, then which individual CYP isoforms were primarily responsible for the catalysis. To accomplish these two objectives, pooled human liver microsomes (HLMS) were used for establishing the CYP-dependent oxidation of *t*-ROH to *t*-RAL. Secondly, selective chemical inhibitors and human cDNA expressed-CYP enzymes (CYP SUPERSOMES) were used for evaluating the significance of individual CYP enzymes in HLMS-catalyzed reactions.

Materials and Methods

Chemicals and CYP Enzymes. *t*-ROH was purchased from Aldrich Chemical Co. (St. Louis, MO). *t*-RAL and *t*-RA were purchased from Sigma Chemical Co. (St. Louis, MO). Furafylline was purchased from Gentest Corp. (Woburn, MA). All other chemicals were purchased either from Aldrich Chemical Co. or from Sigma Chemical Co. Reagents and solvents used were of the highest purity commercially available.

Pooled HLMS and human CYP SUPERSOMES were purchased from Gentest Corp. (Woburn, MA). CYP SUPERSOMES were microsomes prepared from insect cells infected with a baculovirus expression system that codes for a single CYP enzyme plus human P-450 reductase and cytochrome b_5. The control insect microsomes did not contain baculovirus-expressed recombinant CYP protein. HLMS and SUPERSOMES were tested for specific activities and standardized by Gentest. HLMS and SUPERSOMES were aliquoted and stored at −80°C to minimize freeze-thawing cycles.

Oxidation of Retinoids Catalyzed by HLMS or CYP SUPERSOMES. In this study, a concentration of 35 μM *t*-ROH was used for most experiments for two reasons. Firstly, this concentration is within in the range of physiological concentrations of *t*-ROH in human hepatic tissues (11–4000 μM) (Tanumihardjo et al., 1990). Secondly, this concentration permitted facile analyses for metabolite generation.

t-ROH or *t*-RAL was preincubated with HLMS (0.25 mg) or CYP SUPERSOMES (0.025 nmol) in potassium phosphate buffer (0.1 M, pH 7.4) at 37°C in a water bath with continuous shaking for 3 min. Unless specified otherwise, the reaction was initiated by the addition of NADPH (1 mM) to incubation vessels, and the incubation was continued for an additional 20 min. Velocity of the reaction increased linearly during the first 20 min of incubation. The total volume of the incubation mixture was 1 ml. At the end of the incubation, the reaction was terminated by addition of 0.4 ml of ice-cold *n*-butanol/methanol (95:5, v/v). Retinoids were extracted with *n*-butanol/methanol (Shih and Hill, 1991) and were separated by centrifugation (16,000*g* for 30 min at 4°C). The organic phase was collected and stored at −80°C for HPLC analyses. To prevent auto-oxidation and isomerization of retinoids, butylated hydroxytoluene (BHT, 0.5 μmol) was added to the incubation vessels and the incubation and extraction of retinoids were completed in a dark room with yellow light. Incubations of *t*-ROH or *t*-RAL with microsomes prepared from insect cells infected with baculoviruses containing cDNA-expressed human P-450 reductase and human cytochrome b_5 served as controls for CYP SUPERSOMES activities in all experiments. For determinations of kinetic parameters, 9 to 360 μM concentrations of *t*-ROH were used. K_m and V_{max} were determined by linear regression of the raw data and are presented graphically as an Eadie-Hofstee plot. For NAD-dependent conversion of *t*-ROH to *t*-RAL catalyzed by HLMS, NADPH was replaced by 1 mM NAD, and all other conditions were the same as described above.

Inhibition of Oxidation of *t*-ROH and *t*-RAL Catalyzed by HLMS or CYP SUPERSOMES. Experiments designed to assess inhibition by carbon monoxide (CO) followed the same procedures described above except that the incubations were in an atmosphere of CO (80%) and O_2 (20%). The ratio and flow rate of gases were regulated with a gas regulator and incubations opened to air (N_2/O_2, 80:20) served as controls. For chemical inhibition, inhibitors were added to incubation vessels and were preincubated with substrate plus HLMS or CYP SUPERSOMES for 3 min at 37°C before the reactions were initiated by adding NADPH. For mechanism-based inhibition, inhibitors were preincubated with HLMS or CYP SUPERSOMES and NADPH for 15 min at 37°C, and the reactions were initiated by the addition of substrate. Termination of the reactions and extraction of retinoids followed the same procedures as those described above. As suggested by Masimirembwa et al. (1999), a concentration of 10 μM CYP inhibitor was chosen for a one-concentration screen study. Other concentrations were then tested as dictated by the initial results. Incubations without inhibitors served as controls. For heat inactivation experiments, suspensions of HLMS or CYP SUPERSOMES were heated at 100°C for 3 min before addition to incubation vessels.

HPLC Procedures. The solvent delivery system for HPLC consisted of two model 100 A dual piston Beckman pumps and was interfaced with a Shimadzu SPD-10A UV detector (set at a wavelength of 354 nm) and a Shimadzu C-R5A Chromatopac data processor. The HPLC system was equipped with a Beckman mixing chamber and manual injector. Chromatographic conditions described by Kim et al. (1992) were adopted with slight modifications. Analytical eluents consisted of solvent A (acetonitrile/H_2O/acetic acid, 49.75:49.75:0.5, by volume) and solvent B (acetonitrile/H_2O/acetic acid, 90:10:0.04, by volume), both containing 10 mM ammonium acetate. The HPLC elution conditions were as follows: 80% solvent A plus 20% solvent B with a flow rate of 1.2 ml/min for 25 min. Identification and quantitation of retinoids were conducted with two HPLC columns. The first column was a Zorbax octadecylsilane (ODS) column (4.6 × 250 mm) (MAC-MOD Anal. Inc., Chadds Ford, PA) and a flow rate of 1.2 ml/min was used. The second column was a Beckman Ultrasphere Octyl column (2.0 × 250 mm) and a flow rate of 0.2 ml/min was used. One hundred microliters of a mixture of authentic *t*-ROH, *t*-RAL, and *t*-RA or organic supernatant extract of incubation mixtures was loaded onto the HPLC column. Elution times of *t*-RA, *t*-ROH, and *t*-RAL were approximately 14, 16, and 22 min with the Zorbax column and were approximately 18.5, 20.5, and 26.0 min with the Beckman column. Quantitation of retinoids with both HPLC columns was highly consistent. A 50% dilution with HPLC eluent (20% A plus 80% B) of the supernatant before injection on the HPLC column was helpful to achieve a better separation of retinoids. An additional method described by Roberts et al. (1992) was adopted to further confirm the identity of *t*-RAL generated from the reaction. Briefly, HPLC-purified *t*-RAL was vortexed with $NaBH_4$ (a reducing agent for aldehyde, 0.1 mg in methanol) and *t*-RAL was reduced to *t*-ROH. Identity of *t*-ROH was confirmed by HPLC and UV/visible spectroscopy.

Confirmation of *t*-RAL and *t*-RA by Liquid Chromatography-Mass Spectroscopy (LC-MS). *t*-RAL and *t*-RA generated from incubations of *t*-ROH and *t*-RAL plus HLMS were confirmed by LC-MS using a fully integrated Hewlett-Packard Series 1100 LC/mass selective detector system (Hewlett-Packard, Palo Alto, CA). The HPLC system, composed of a binary solvent pump, a vacuum degasser, and a temperature-controlled autosampler and column compartment, was serially interfaced to an Hewlett-Packard 1100 diode array detector (DAD) and mass selective detector quadrupole mass spectrometer. A Beckman Ultrasphere Octyl column (2.2 mm i.d. × 250 mm, 5-μm particle size) was used and operated under the isocratic conditions described above at a flow rate of 0.200 ml/min using a sample injection volume of 10 μl. The column effluent was subjected to positive mode electrospray ionization using nitrogen as a drying gas at a temperature of 350°C and a flow rate of 10.0 liters/min with a nebulizer pressure of 25 psi and a capillary voltage of 4 kV. Signal responses for the analytes were optimized as a function of fragmentor voltage resulting in a setting of 50 V for all analytes. The selection of ion windows, span (±0.3 Da), and dwell (443 ms/ion) for selected ion monitoring data acquisition and processing was accomplished using

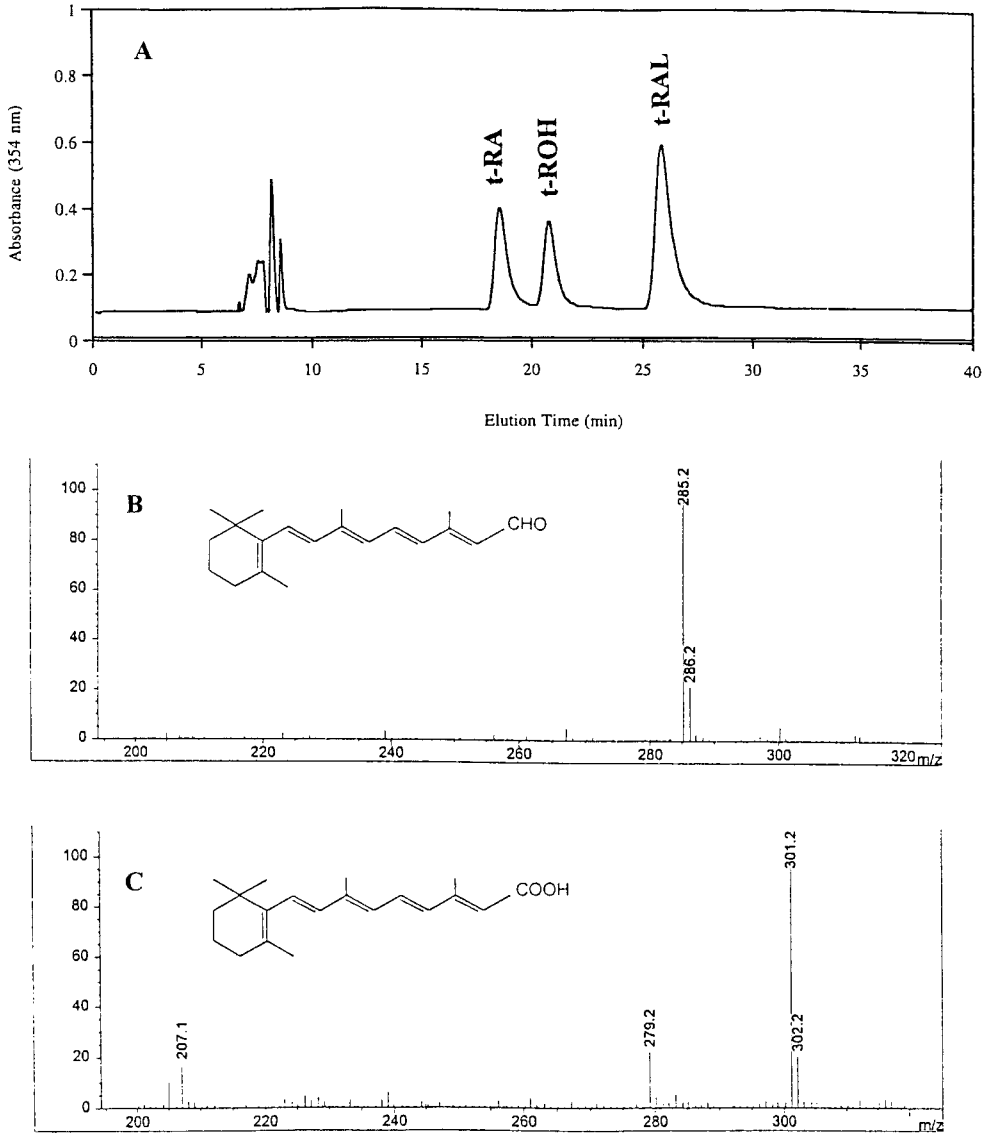

FIG. 1. *HPLC profiles of authentic t-RA, t-ROH, and t-RAL from a Beckman Ultrasphere Octyl column (2.2 mm i.d. × 250 mm, 5-μm particle size) obtained at 354 nm (A); mass spectra of authentic t-RAL (B); and t-RA (C).*

For chromatographic and LC-MS conditions, see *Materials and Methods.*

Hewlett-Packard ChemStation software operating in the high resolution mode. Ions monitored were *m*/z 285.2 and 301.2, corresponding to the $[M+H]^+$ for *t*-RAL and *t*-RA, respectively.

Demethylation of Imipramine. Imipramine demethylation was conducted in reaction vessels containing potassium phosphate buffer (0.1 M, pH 7.4) and 0.1 mM imipramine as substrate. HLMS or CYP SUPERSOMES were preincubated with imipramine at 37°C for 3 min. Final volumes of the incubation mixtures were 0.5 ml. Reactions were initiated by the addition of 1 mM NADPH and were continued for 20 min. The reactions were terminated by freezing, and imipramine metabolites were extracted according to the methods described by Sequeira and Strobel (1995). Briefly, 0.25 ml of Na_2CO_3 (2 M, pH 12) was added to the incubation vessels and mixed well. Ethyl ether (2.5 ml) was added to the vessels and vortexed. The incubation mixtures were centrifuged at 3000*g* for 10 min. The ether layer was decanted and back-extracted into 0.5 ml HCl (0.1 M). Extraction efficiency for the demethylated metabolite was approximately 60 to 68% (Sequeira and Strobel, 1995). After extraction, the ether layer was decanted and dried under N_2. The HPLC mobile phase (500 μl) was used for suspension of the metabolites.

HPLC Analyses of Metabolites of Imipramine Oxidation. With the same solvent delivery system described previously, identification and quantitation of desipramine were conducted with a Supelco LC-PCN column (5 μm, 250 × 4.6 mm) (Supelco, Supelco Park, Bellefonte, PA) following the procedures described by Sequeira and Strobel (1995). Metabolites of imipramine oxidation were separated by HPLC then identified by matching elution times with the standard compounds. The mobile phase was pumped at a flow rate of 1.4 ml/min and consisted of acetonitrile/methanol/K_2HPO_4 (10 mM, pH 7.0) = 40:30:25, and the UV detector was set at 214 nm.

Statistical Analyses. All experimental data were expressed as means ± S.D. for three or four experimental measurements. A Microsoft Excel statistics package (version 5.0, Microsoft Corp., Redmond, WA) was used for all statistical analyses.

Results

Identifications and Quantitations of *t*-RAL. An HPLC chromatogram of authentic *t*-RA, *t*-ROH, and *t*-RAL is shown in Fig. 1A. Under the chromatographic conditions used, *t*-ROH was completely separated from *t*-RAL and *t*-RA, thus quantitations of each individual retinoid were readily achieved. The mass spectra of authentic *t*-RAL and *t*-RA (metabolites of oxidative conversion of *t*-ROH) are pre-

TABLE 1

Oxidative conversion of t-ROH to t-RAL catalyzed by HLMS[1]

t-ROH (35 μM) was preincubated with HLMS (0.18 mg) or heat-inactivated (boiled) HLMS (100°C for 3 min) at 37°C for 3 min in the dark. Reactions were initiated by additions of NADPH (1 mM) and were continued for 15 min in an atmosphere of air. Catalytic activity of HLMS was evaluated with incubation of HLMS plus imipramine and demethylase activity of HLMS was 900 pmol/min/mg protein. Results are means ± S.D. of three to four measurements. Statistical differences between values were evaluated with *t* tests ($P < .05$). For more details, see *Materials and Methods.*

Enzyme Source	Cofactor (1 mM)	CO/O_2 (80:20)	Specific Activity
			pmol/min/mg protein
HLMS	NADPH	−	43.5 ± 2.7
HLMS	NADH	−	27.5 ± 0.8
HLMS	NADPH[a]	−	48.2 ± 3.1
HLMS	−	−	ND[b]
HLMS	NADPH	+	4.8 ± 1.6
Boiled HLMS	NADPH	−	ND

[a] NADPH was produced from an NADPH-regenerating system containing NADP (0.5 mM), glucose-6-phosphate (5 mM), glucose-6-phosphate dehydrogenase (4 U/ml), and MgCl (10 mM).
[b] ND indicates that values were below the detection limit (1 ng/100 μl).

sented in Fig. 1, B and C, respectively. The major ion fragments were detected at 285.2 and 301.2 *m/z*, resulting from the positive ionization of *t*-RAL and *t*-RA ($[M+H]^+$), respectively. Detection of $[M+H]^+$ at 285.2 and 301.2 *m/z* were then used for confirmation of the presence of *t*-RAL and *t*-RA in incubation mixtures.

Characterizations of HLMS-Catalyzed Oxidation of *t*-ROH. The HLMS-catalyzed oxidation of *t*-ROH to *t*-RAL was characterized and the results are presented in Table 1. The reaction was catalyzed after additions of either NADPH or NADH, but NADPH appeared to be a much more effective cofactor than NADH. Omission of these cofactors resulted in undetectable reactions. The reaction was also abolished with heat inactivation and was strongly inhibited by carbon monoxide (80:20 CO/O_2 versus 80:20 N_2/O_2). Activity after addition of an NADPH-regenerating system was higher but not statistically different from that observed with direct additions of NADPH alone.

Figure 2 shows that the reaction velocity of the HLMS-catalyzed conversion of *t*-ROH to *t*-RAL was proportional to amounts of HLMS protein in the incubation vessels. As concentrations of HLMS protein increased (0–1.0 mg), the velocity of the reaction increased linearly ($r^2 = 0.997$). For all subsequent experiments with HLMS, protein concentrations were within the linear range.

Figure 3A presents an Eadie-Hofstee plot of the NADPH-dependent conversion of *t*-ROH to *t*-RAL catalyzed by HLMS. K_m and V_{max} values were 19.4 μM and 52 pmol/min/mg protein, respectively. For comparison purposes, an Eadie-Hofstee plot for the NAD-dependent conversion of *t*-ROH to *t*-RAL catalyzed by HLMS is also presented in Fig. 3B and the K_m and V_{max} values were 41.5 μM and 280 pmol/min/mg protein, respectively.

Chemical Inhibition of HLMS-Catalyzed Oxidation of *t*-ROH. Table 2 presents the effects of selective CYP inhibitors on the HLMS-catalyzed oxidation of *t*-ROH to *t*-RAL. At final concentrations of 10 μM, selective inhibitors for CYP2A6, CYP2B6, or CYP2E1 did not produce significant effects on the reaction. On the other hand, selective inhibitors for CYP family 1 (CYP1A1, CYP1A2, and CYP1B1), the CYP2C and CYP3A subfamilies, and CYP2D6 each produced significant inhibitory effects on reaction rates. Among them, furafylline (highly selective for CYP1A2) and troleandomycin (TAO; highly selective for CYP3A isoforms) each produced profound inhibitory effects on the HLMS-catalyzed oxidation of *t*-ROH to *t*-RAL (70–75% inhibition).

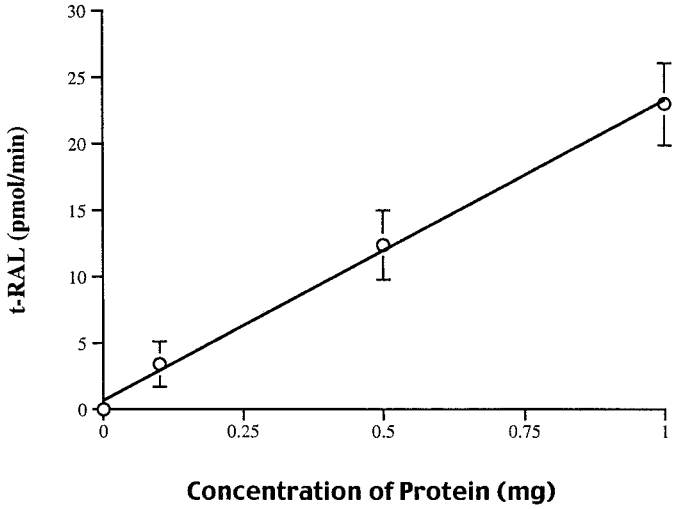

FIG. 2. *Effect of concentration of protein on velocity of HLMS-catalyzed oxidation of t-ROH to t-RAL.*

t-ROH (35 μM) was incubated with HLMS (0.0–1.0 mg of protein) plus NADPH (1 mM) in potassium phosphate buffer (0.1 M, pH 7.4) at 37°C for 20 min in the dark. Results are means ± S.D. of three to four measurements. For details, see *Materials and Methods*.

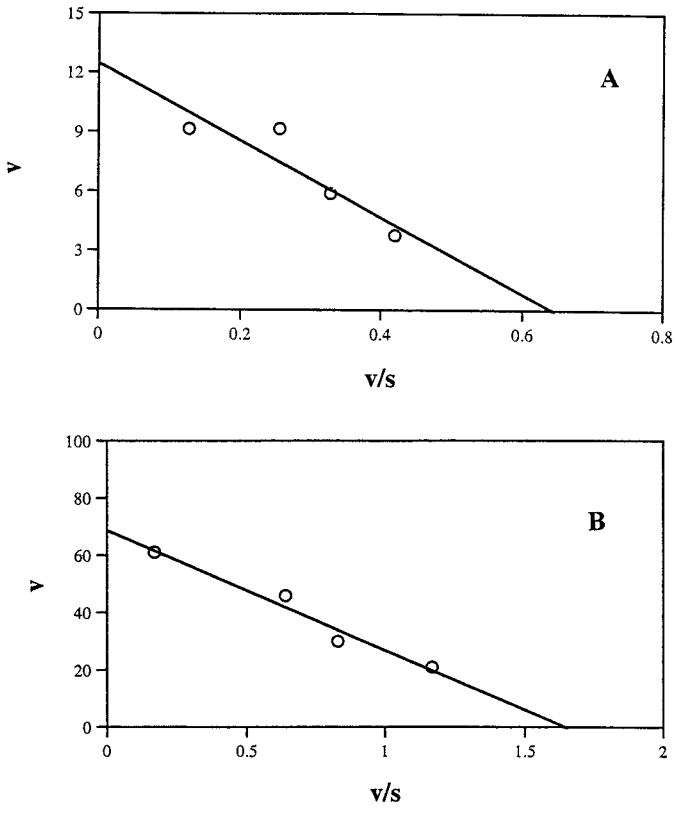

FIG. 3. *Eadie-Hofstee plots of NADPH-dependent (A) and NAD-dependent (B) conversion of t-ROH to t-RAL in human hepatic microsomes.*

K_m and V_{max} for NADPH-dependent reaction were 19.4 μM and 52 pmol/min/mg protein ($r^2 = 0.77$). K_m and V_{max} for NAD-dependent reaction were 41.5 μM and 280 pmol/min/mg protein ($r^2 = 0.96$).

To substantiate the observed inhibition produced by furafylline, TAO, ANF, quinidine, quercetin, sulfaphenazole, and tranylcypromine, two additional concentrations (1 and 100 μM) of these inhibitors were investigated for their inhibitory effects and the results are

TABLE 2

Effects of selective inhibitors on HLMS-catalyzed conversion of t-ROH to t-RAL

t-ROH (35 μM) was preincubated with HLMS (0.25 mg) plus inhibitors (10 μM) in potassium phosphate buffer (0.1 M, pH 7.4) at 37°C for 3 min in the dark. Reactions were initiated by addition of NADPH (1 mM) and continued for 20 min. Results are means ± S.D. of three to four measurements. Statistical differences between control and control plus inhibitor were evaluated with *t* tests ($P < .05$). For more details, see *Materials and Methods.*

Inhibitor (10 μM)	Inhibition Selectivity	% Control[a]
ANF	Family 1	65 ± 7.8
Furafylline[b]	CYP1A2	25 ± 5.7
DDC	CYP2A6, CYP2E1	124 ± 16
Orphenadrine[b]	CYP2B6	102 ± 4
Quercetin	CYP2C8	75 ± 5.3
Sulfaphenazole	CYP2C9	58 ± 2.4
Tranylcypromine	CYP2C19	60 ± 1.2
Quinidine	CYP2D6	65 ± 3.7
TAO[b]	CYP3A subfamily	30 ± 1.5

[a] Specific activity for control was 35.7 ± 2.7 pmol/min/mg protein.
[b] Mechanism-based inhibitors and preincubation with HLMS plus NADPH was required.

presented in Fig. 4. At concentrations of either 1 or 100 μM, effects produced by these concentrations did not distinguish the inhibitors, suggesting that those chemical inhibitors did not exhibit selectivity at those two concentrations.

CYP SUPERSOMES-Catalyzed Conversions of *t*-ROH to *t*-RAL and *t*-RAL to *t*-RA. To further ensure that the CYP SUPERSOMES used in the study were enzymatically active and to standardize the activities, CYP SUPERSOMES were incubated with imipramine under the same reaction conditions as those used for retinoid biotransformation. Activities of CYP SUPERSOMES for demethylating imipramine to desipramine are presented in Fig. 5. All CYP SUPERSOMES investigated in this study exhibited readily measurable imipramine demethylase activities.

Activities of CYP SUPERSOMES for catalyzing oxidation of *t*-ROH to *t*-RAL were then assessed and the results are presented in Fig. 6. CYP1A1, CYP1A2, CYP1B1, CYP3A5, CYP3A4, and CYP2D6 SUPERSOMES exhibited relatively high catalytic activities for oxidation of *t*-ROH to *t*-RAL by comparison with their relatively low imipramine demethylase activities; i.e., ratios of *t*-ROH oxidation to imipramine demethylation were comparatively high for these CYP isoforms. Interestingly and in contrast, CYP2C18 and CYP2C19 SUPERSOMES, which were highly active in the catalysis of imipramine demethylation, showed only minimal catalytic activities for conversion of *t*-ROH to *t*-RAL.

Table 3 exhibits kinetic constants for CYP1A1, CYP1A2, CYP1B1, CYP2D6, and CYP3A4 SUPERSOMES-catalyzed conversion of *t*-ROH to *t*-RAL. CYP1A1, CYP1A2, and CYP1B1 exhibited relatively low K_m and high V_{max} values. The K_m for CYP3A4 was higher than the K_m for CYP1A1, CYP1A2, or CYP1B1, but much lower than the K_m for CYP2D6. To further substantiate the observations shown in Fig. 6, catalysis of oxidation of *t*-RAL to *t*-RA by the same CYP SUPERSOMES also was investigated and the results are presented in Fig. 7. CYP1A1 and CYP1A2 SUPERSOMES exhibited impressive catalytic activities for conversion of *t*-RAL to *t*-RA whereas other CYP SUPERSOMES showed only minimal activities for catalyzing the same reaction.

Discussion

This study has shown for the first time that P-450 cytochromes in human adult hepatic microsomes will catalyze oxidative conversion of *t*-ROH to *t*-RAL. The identity of *t*-RAL generated from incubations of *t*-ROH plus HLMS was confirmed with HPLC, LC-MS, and reduction of *t*-RAL generated to *t*-ROH by reducing agent ($NaBH_4$). The catalysis was enzymatic as evidenced from observations that the HLMS-dependent reaction was terminated by heat inactivation and also exhibited substrate saturation. Evidence also strongly indicated that this reaction was catalyzed primarily by CYP enzymes because the reaction was NADPH-dependent and was strongly inhibited by CO as well as by various other CYP inhibitors. It is known that CYP can catalyze conversions of a variety of primary or secondary alcohols to aldehydes or ketones through formation of gem-diols with subsequent dehydration to a keto group (Parkinson, 1996). Because *t*-ROH is a primary alcohol, CYP-catalyzed conversion of *t*-ROH to *t*-RAL may also proceed via the same mechanism.

Recent studies have indicated that hepatic concentrations of total retinoid alcohols could be as high as 2860 nmol/g liver (approximately 4 mM) (Tanumihardjo et al., 1990; Barua et al., 1997). As shown in this study, the apparent K_m and V_{max} values for the NADPH-

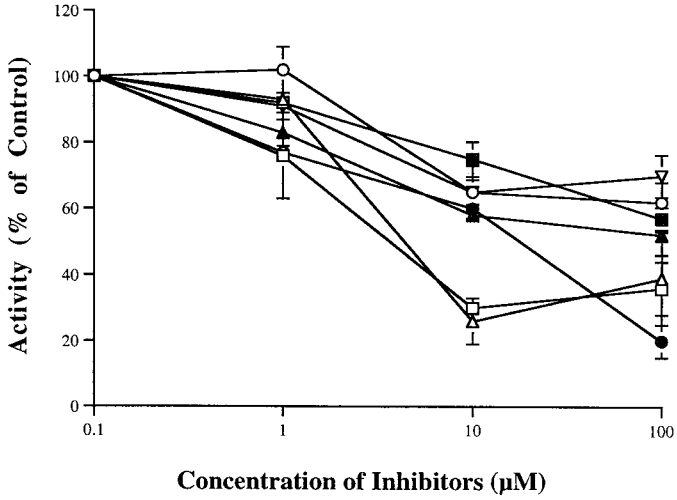

FIG. 4. *Effects of varying concentrations of chemical inhibitors on HLMS-catalyzed oxidation of t-ROH to t-RAL.*

ANF (○), furafylline (Δ), TAO (■), tranylcypromine (●), sulfaphenazole (▲), quercetin (■), or quinidine (▽) were incubated with *t*-ROH (35 μM), HLMS (0.25 mg protein), and NADPH (1 mM) in potassium phosphate buffer (0.1 M, pH 7.4) at 37°C for 20 min in the dark. Results are means ± S.D. of three to four measurements. Statistical differences between control and control plus inhibitor were evaluated with *t* tests ($P < .05$). For details, see *Materials and Methods*.

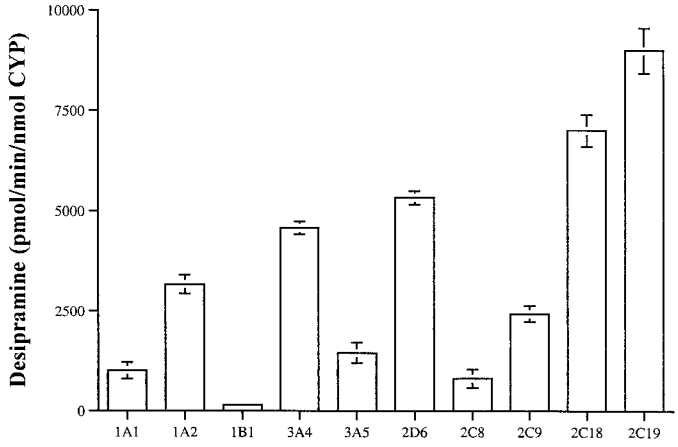

FIG. 5. *Demethylation of imipramine catalyzed by CYP SUPERSOMES.*

Imipramine (0.1 mM) was incubated with CYP SUPERSOMES (0.025 nmol) plus NADPH (1 mM) in potassium phosphate buffer (0.1 M, pH 7.4) at 37°C for 20 min. Results are means ± S.D. of three to four measurements. For details, see *Materials and Methods*.

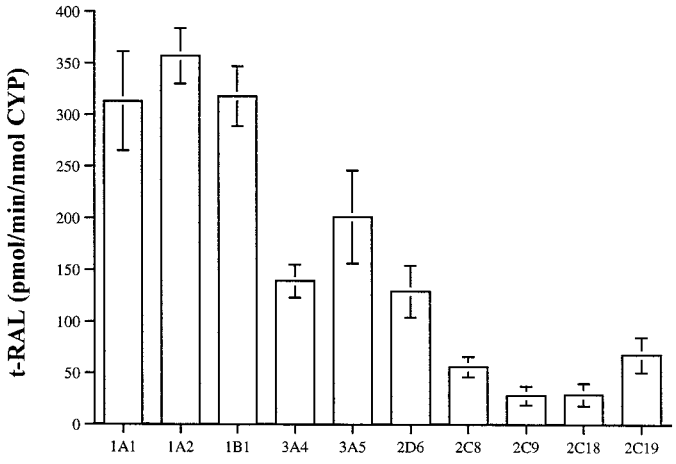

FIG. 6. *Conversion of t-ROH to t-RAL catalyzed by CYP SUPERSOMES.*

t-ROH (35 μM) was incubated with CYP SUPERSOMES (0.025 nmol) plus NADPH (1 mM) in potassium phosphate buffer (0.1 M, pH 7.4) at 37°C for 20 min in the dark. Results are means ± S.D. of three to four measurements. For details, see *Materials and Methods*.

TABLE 3

Kinetic constants for oxidation of all-trans-retinol to all-trans-retinal catalyzed by CYP isoforms

t-ROH was incubated with CYP isoforms (0.025 nmol) in potassium phosphate buffer (0.1 M, pH 7.5) at 37°C for 20 min in total darkness. For further details, *see Materials and Methods.*

CYP	Apparent K_m	V_{max}
	μM	*pmol/min/nmol CYP*
1A1	8	507
1A2	9	491
1B1	11	493
2D6	67	193
3A4	25	225

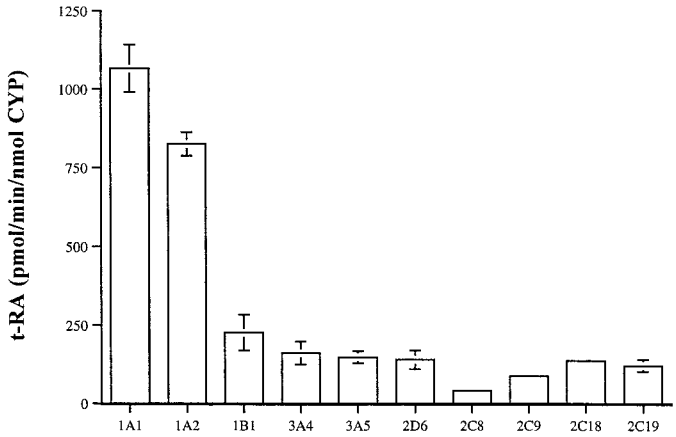

FIG. 7. *Conversion of t-RAL to t-RA catalyzed by CYP SUPERSOMES.*

t-RAL (35 μM) was incubated with CYP SUPERSOMES (0.025 nmol) plus NADPH (1 mM) in potassium phosphate buffer (0.1 M, pH 7.4) at 37°C for 20 min in the dark. Results are means ± S.D. of three to four measurements. For details, see *Materials and Methods*.

dependent, HLMS-catalyzed conversion of *t*-ROH to *t*-RAL were approximately 19.4 μM and 52 pmol/min/mg protein, respectively. Interestingly, the NAD-dependent, HLMS-catalyzed conversion of *t*-ROH to *t*-RAL exhibited a higher K_m (41.5 μM) and a higher V_{max} (280 pmol/min/mg protein). Because hepatic concentrations of retinol are far higher than either K_m, V_{max} is indicative of the catalytic efficiency. Therefore, NAD-dependent catalysis appeared to be a major pathway in human hepatic microsomal synthesis of *t*-RAL from *t*-ROH. This observation is consistent with the current concept that microsomal retinol dehydrogenases are the primary catalysts for converting *t*-ROH to *t*-RA in the liver (Napoli and Race, 1990; Kim et al., 1992; Napoli et al., 1992; Blaner and Olson, 1994; Napoli, 1996; Gough et al., 1998).

However, CYP-dependent oxidation of *t*-ROH to *t*-RAL may be important for hepatic and/or extrahepatic biosynthesis of *t*-RA. The newly identified CYP-dependent oxidation of *t*-ROH and *t*-RAL could represent an important alternative mechanism for biosynthesis of both *t*-RAL and *t*-RA in vivo. Recent studies in vivo appear to support the important roles of CYP enzymes in hepatic retinoid metabolism. For example, knockout of aryl hydrocarbon receptor, which regulates genes encoding CYP1A1, CYP1A2, and CYP1B1, resulted in significant changes of hepatic levels of retinoids in mice (Andreola et al., 1997; Gonzalez and Fernandez-Salguero, 1998). In addition, under conditions in vivo, CYP enzymes are likely to be saturated by hepatic *t*-ROH. Because many CYP enzymes also catalyze metabolisms of various human drugs, potential interactions between retinoids and drugs might have pharmaceutical and toxicological significance.

Most P-450 enzymes involved in xenobiotic biotransformation, such as CYP3A4, members of the CYP2C subfamily, CYP2D6, and 1A2, are primarily localized in liver endoplasmic reticulum (microsomes) (Parkinson, 1996). Some P-450 enzymes, such as CYP1A1 and CYP1B1, are mainly expressed in extrahepatic tissues. For example, CYP1A1 is readily detected in lung, intestine, skin, lymphocytes, and placenta (Parkinson, 1996) whereas CYP1B1 is preferentially expressed in hormone-synthesizing organs such as adrenal gland, ovaries, and testes (Juchau et al., 1998).

Catalytic roles for individual CYP enzymes were explored by evaluating the effects of selective inhibitors on the HLMS-dependent oxidation of *t*-ROH to *t*-RAL. On the basis of chemical inhibition in hepatic microsomes, members of CYP family 1 and CYP3A subfamily appeared to be quite active whereas members of CYP2C subfamily appeared to be much less active. CYP2A6, CYP2B6, and CYP2E1 exhibited virtually no detectable activity. However, the sole application of chemical inhibition became problematic for further identifying particular CYP enzymes primarily responsible for catalyzing the reaction. This is because many chemical inhibitors available are selective but not specific. Indeed, most of them can inhibit more than one CYP enzyme (Parkinson, 1996). To help address this problem, cDNA-expressed human CYP enzymes (CYP SUPERSOMES) were also used for assessing rates of the reaction catalyzed by individual CYP enzymes. Results from CYP SUPERSOMES complemented the data obtained from chemical inhibition, and thus assisted in identifying the CYP enzymes most responsible for catalyzing the reaction in human adult liver microsomes. To assure that the CYP SUPERSOMES used were enzymatically active and to standardize activities, demethylation of imipramine catalyzed by CYP SUPERSOMES was conducted under the same reaction conditions as those used for studies of retinoid oxidation. Imipramine is a common substrate for members of CYP family 1, for CYP2C and CYP3A subfamilies, and for CYP2D6 (Parkinson, 1996) and a body of information pertaining to these activities is now available. Imipramine demethylase activity, therefore, can serve as an indicator for comparative catalytic activities in CYP SUPERSOMES. Ratios of imipramine demethylation to *t*-ROH oxidation thus provided important information pertaining to the capacity of individual CYP isoform to catalyze *t*-RA biosynthesis.

CYP1A2 SUPERSOMES exhibited a relatively low K_m and high V_{max} for conversion of *t*-ROH to *t*-RAL. In human adult liver,

CYP1A2 accounts for approximately 18% of total CYP enzymes (Parkinson, 1996). Both high catalytic activity and a relatively high hepatic concentration strongly suggest that CYP1A2 acts as one of the major CYP enzymes to catalyze the oxidation of *t*-ROH to *t*-RAL in hepatic microsomes. This is consistent with the observation that furafylline, a highly selective inhibitor of CYP1A2 (Racha et al., 1998), produced strong inhibition (70–75%) of the HLMS-catalyzed reaction. ANF exhibited less potency in blocking CYP1A2-catalyzed conversion of *t*-ROH to *t*-RAL than furafylline. At the same concentration (10 μM), ANF produced only approximately 35% inhibition. The relatively low inhibitory potency of ANF was confirmed by comparing the effects of ANF and furafylline on CYP1A2 SUPERSOMES-catalyzed reactions.

CYP3A4 and CYP3A5 SUPERSOMES also showed relatively high activities (roughly 150–200 pmol/min/nmol) for catalyzing conversion of *t*-ROH to *t*-RAL. When hepatic levels of the CYP3A subfamily (approximately 40% of total hepatic CYP enzymes) are taken into account, it appears that the CYP3A subfamily would also play an important role for catalyzing the reaction in adult human liver. The fact that TAO effectively inhibited the HLMS-catalyzed reaction appeared to support this assessment. In this regard, separate experiments showed that TAO also inhibited the CYP1A2 SUPERSOMES-catalyzed reaction by 20 to 25% at 10-μM concentrations, indicating that part of the inhibitory effect produced by TAO on the HLMS-catalyzed reaction was due to inhibition of CYP1A2 activity.

Although CYP2D6 SUPERSOMES were also active for catalyzing the reaction, its relatively low concentration (approximately 2% of total hepatic CYP enzymes) suggested that CYP2D6 was not a major factor for conversion of *t*-ROH to *t*-RAL in human adult liver. This conclusion also was supported by the observation that quinidine produced only a moderate inhibitory effect (approximately 35% inhibition) at a relatively high (10 μM) concentration on the HLMS-catalyzed conversion of *t*-ROH to *t*-RAL.

CYP2C8, CYP2C9, CYP2C18, and CYP2C19 SUPERSOMES each exhibited minimal activities ($<$100 pmol/min/nmol) for catalyzing conversion of *t*-ROH to *t*-RAL, which sharply contrasted with their outstandingly high imipramine demethylase activities (1000–30,000 pmol/min/nmol). This observation suggested that *t*-ROH was not a good substrate for CYP2C subfamily isoforms in terms of oxidation to *t*-RAL and that members of CYP2C subfamily were not likely to be quantitatively important in catalyzing the reaction in human adult liver. The moderate inhibitory effects produced by inhibitors of CYP2C in HLMS-catalyzed reactions were probably the sum of inhibition of activities of all four CYP2C isoforms as well as nonspecific inhibition of activities of other CYP enzymes.

As *t*-RAL can be rapidly oxidized to *t*-RA, the lower generation of *t*-RAL via oxidation of *t*-ROH catalyzed by CYP2D6 or members of the CYP2C subfamily might also be the result of their potential activities for catalyzing conversion of *t*-RAL to *t*-RA. As shown in Fig. 7, however, CYP2D6, CYP2C8, CYP2C9, CYP2C18, and CYP2C19 all showed relatively low activities for catalysis of oxidation of *t*-RAL to *t*-RA. For these CYP enzymes, therefore, the lower generations of *t*-RAL shown in Fig. 6 appeared due to their lower catalytic capacities for converting *t*-ROH to *t*-RAL.

CYP1A1 and CYP1B1 SUPERSOMES exhibited very high catalytic activities for conversion of *t*-ROH to *t*-RAL as well as low K_m values. Because both CYP1A1 and CYP1B1 are expressed at only very low constitutive levels in human adult liver, they are not likely to act as significant participants in hepatic biosynthesis of *t*-RA from *t*-ROH. However, in various extrahepatic tissues (such as in brain and fetal tissues), expressions of CYP1A1 and CYP1B1 are readily detected, particularly after exposures to inducing agents (Strobel et al., 1997; Juchau et al., 1998). Therefore, CYP1A1 and CYP1B1 may perform important roles in tissue-specific biosynthesis of *t*-RA from *t*-ROH. CYP1A1 and CYP1B1 are highly inducible by environmental chemicals (Parkinson, 1996) and such induction might remarkably increase the rates of biosynthesis of *t*-RA catalyzed by CYP1A1 and CYP1B1 in human fetal tissues, thereby influencing normal development. On the other hand, as substrates for CYP1A1 and CYP1B1, retinoids might also inhibit xenobiotic oxidation catalyzed by these two enzymes. Indeed, inhibition by retinol of CYP1A1-catalyzed xenobiotic oxidation reactions has been reported recently (Yamazaki and Shimada, 1999).

Conversion of *t*-RAL to *t*-RA catalyzed by CYP SUPERSOMES also was investigated to corroborate investigations with HLMS. CYP1A1 and CYP1A2 SUPERSOMES were highly active for catalyzing conversion of *t*-RAL to *t*-RA as has also been reported previously (Roberts et al., 1992; Raner et al., 1996). With catalysis by CYP1A1 and CYP1A2 SUPERSOMES, rates of oxidation of *t*-RAL to *t*-RA were roughly 2- to 3-fold greater than that of oxidation of *t*-ROH to *t*-RAL, suggesting that the latter was the rate-limiting step for biosynthesis of *t*-RA from *t*-ROH when catalyzed by these enzymes. Interestingly, for the CYP1B1, CYP3A4, CYP3A5, and CYP2D6 SUPERSOMES-catalyzed reactions, conversion of *t*-ROH to *t*-RAL appeared not to be the rate-limiting step because rates of oxidation of *t*-ROH to *t*-RAL were roughly the same as those of oxidation of *t*-RAL to *t*-RA. Similar to their catalysis of the conversion of *t*-ROH to *t*-RAL, CYP SUPERSOMES of members of CYP2C subfamily showed minimal activities in catalyzing conversion of *t*-RAL to *t*-RA.

In summary, the conversion of *t*-ROH to *t*-RAL catalyzed by P-450 cytochromes in human adult hepatic microsomal fractions indicated that CYP1A2 and CYP3A4 appear to be the primary enzymes responsible for catalyzing *t*-RA biosynthesis in human adult hepatic microsomes. Because of their excellent catalytic activities, low K_m values, and high inducibility by environmental chemicals and xenobiotics, CYP1A1 and CYP1B1 could play important roles in human extrahepatic and fetal tissue-specific biosynthesis of *t*-RA from *t*-ROH.

References

Andreola F, Fernandez-Salguero P, Chiantore MV, Petkovich MP, Gonzalez FJ and De Luca LM (1997) Aryl hydrocarbon receptor knockout mice (AHR$^{-/-}$) exhibit liver retinoid accumulation and reduced retinoic acid metabolism. *Cancer Res* **57:**2835–2838.

Barua AB, Duitsman PK, Kostic D, Barua M and Olson JA (1997) Reduction of serum retinol levels following a single oral dose of all-trans-retinoic acid in humans. *Int J Vitam Nutr Res* **67:**423–426.

Blaner WS and Olson JA (1994) *The Retinoids*, 2nd ed. (Sporn MB, Roberts AB and Goodman DS eds) pp 229–255, Raven Press, New York.

Duester G (1998) Alcohol dehydrogenase as a critical mediator of retinoic acid synthesis from vitamin A in the mouse embryo. *J Nutr* **128 (Suppl 2):**459s–462s.

Gonzalez FJ and Fernandez-Salguero P (1998) The aryl hydrocarbon receptor studies using the AHR-null mice. *Drug Metab Dispos* **26:**1194–1198.

Gough WH, VanOoteghem S, Sint T and Kedishvili NY (1998) cDNA cloning and characterization of a new human microsomal NAD$^+$-dependent dehydrogenase that oxidizes all-trans-retinol and 3α-hydroxysteroids. *J Biol Chem* **273:**19778–19785.

Juchau MR, Boutelet-Bochan H and Huang Y (1998) Cytochrome-P450-depdendent biotransformation of xenobiotics in human and rodent embryonic tissues. *Drug Metab Rev* **30:**541–568.

Kim C-I, Leo MA and Lieber CS (1992) Retinol forms retinoic acid via retinal. *Arch Biochem Biophys* **294:**388–393.

Masimirembwa CM, Otter C, Berg M, Jonsson M, Leidvik B, Jonsson E, Johansson T, Backman A, Edlund A and Andersson TB (1999) Heterologous expression and kinetic characterization of human cytochromes P-450: Validation of a pharmaceutical tool for drug metabolism research. *Drug Metab Dispos* **27:**1133–1142.

Means AL and Gudas LJ (1995) The roles of retinoids in vertebrate development. *Annu Rev Biochem* **64:**201–233.

Napoli JL (1996) Retinoic acid biosynthesis and metabolism. *FASEB J* **10:**993–1001.

Napoli JL, Posch KC and Burns RD (1992) Microsomal retinal synthesis: Retinol vs. holo-crbp as substrate and evaluation of NADP, NAD, and NADPH as cofactors. *Biochim Biophy Acta* **1120:**183–186.

Napoli JL and Race KR (1990) Microsomes convert retinol and retinal into retinoic acid and interfere in the conversions catalyzed by cytosol. *Biochim Biophy Acta* **1034:**228–232.

Parkinson A (1996) *Toxicology, the Basic Science of Poisons*, 5th ed. (Klaassen CD ed) pp 113–186, McGraw-Hill, New York.
Petcovich M, Nigel JB, Krust A and Chambon P (1987) A human retinoic acid receptor which belongs to the family of nuclear receptors. *Nature (Lond)* **330:**444–450.
Racha JK, Rettie AE and Kunze KL (1998) mechanism-based inactivation of human cytochrome P450 1A2 by furafylline: Detection of a 1:1 adduct to protein and evidence for the formation of a novel imidazomethide intermediate. *Biochemistry* **37:**7407–7419.
Raner GM, Vaz ADN and Coon MJ (1996) Metabolism of all-trans, 9-cis, and 13-cis isomers of retinal by purified isozymes of microsomal cytochrome P-450 and mechanism-based inhibition of retinoid oxidation by citral. *Mol Pharmacol* **49:**515–522.
Roberts ES, Vaz ADN and Coon MJ (1992) Role of isozymes of rabbit microsomal cytochrome P-450 in the metabolism of retinoic acid, retinol, and retinal. *Mol Pharmacol* **41:**427–433.
Sequeira DJ and Strobel HW (1995) High performance liquid chromatographic method for the analysis of imipramine metabolism *in vitro* by liver and brain microsomes. *J Chromatogr B: Biomed Appl* **673:**251–258.
Shih TW and Hill DL (1991) Conversion of retinol to retinal by rat liver microsomes. *Drug Metab Dispos* **19:**332–335.
Soprano DR and Soprano KJ (1995) Retinoids as teratogens. *Annu Rev Nutr* **15:**111–132.
Strobel HW, Geng J, Kawashima H and Wang H (1997) Cytochrome P450-dependent biotransformation of drugs and other xenobiotic substrates in neural tissues. *Drug Metab Rev* **29:**1079–1105.
Tanumihardjo SA, Furr HC, Amed'ee MO and Olson JA (1990) Retinyl ester (vitamin A ester) and carotenoid composition in human liver. *Int J Vitam Nutr Res* **60:**307–313.
Yamazaki H and Shimada T (1999) Effects of arachidonic acid, prostaglandins, retinol, retinoic acid and cholecalciferol on xenobiotic oxidations catalyzed by human P450 enzymes. *Xenobiotica* **29:**231–241.